ACS APPLIED MATERIALS & INTERFACES

www.acsami.org

Research Article

H_2-Promoted Benign Coke Strategy for Dimethyl Ether Carbonylation with Long-Term Stability and High Activity

Dong Fan, Nan Chen, Songyue Han, Lingyun Li, Nan Wang, Wenhao Cui, Quanyi Wang, Peng Tian,* and Zhongmin Liu*

Cite This: *ACS Appl. Mater. Interfaces* 2024, 16, 18745−18753

Read Online

ACCESS | Metrics & More | Article Recommendations | Supporting Information

ABSTRACT: Zeolite-catalyzed dimethyl ether (DME) carbonylation provides a novel route to producing methyl acetate (MeOAc). Mordenite (MOR) has drawn significant interest because of its remarkable MeOAc selectivity in DME carbonylation, albeit with limited catalytic stability. Herein, novel MOR-based DME carbonylation catalysts, distinguished by long-term stability and high activity were successfully developed, based on an H_2-promoted benign coke strategy. Both the H_2 cofeeds and the presence of metal species with hydrogenation capability are demonstrated to be crucial for the regulation of coke depositions. The coke deposits can potentially cover the acid sites in the 12-MR main channels, thereby mitigating the occurrence of undesirable methanol-to-hydrocarbon side reactions. Meanwhile, the elimination of ultralarge coke species under the assistance of H_2 and Cu species could ensure smooth mass transfer within the catalyst, contributing to its remarkable catalytic performance. The most highlighted DME carbonylation performance was achieved on coke-mediated CuZn-HMOR with a high MeOAc yield of 0.4−0.5 $g \cdot g_{cat}^{-1} \cdot h^{-1}$ for over 520 h (over 50× enhancement versus HMOR), exhibiting promising industrial application potential. The current strategy is expected to inspire further research into zeolite-catalyzed reactions, which could be potentially improved by the presence of benign coke.

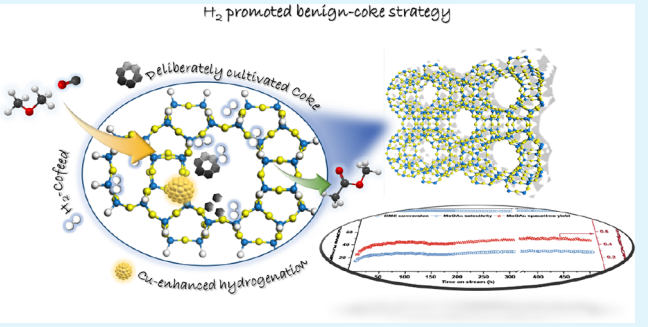

KEYWORDS: *DME carbonylation, precoking, mordenite, zeolite, heterogeneous catalysis*

1. INTRODUCTION

Dimethyl ether (DME) carbonylation over zeolite catalysts provides an effective route for the valorization of C1 chemicals.[1,2] The process has attracted significant attention from both academia and industry because DME could be readily produced via syngas from nonpetroleum resources, such as natural/shale gas, coal, or biomass.[3−5] Methyl acetate (MeOAc), the highly selective product of DME carbonylation, could be further hydrogenated to produce ethanol,[6,7] an important building block for chemicals and an ideal additive for transportation fuels. In fact, a commercial DMTE (DME-to-ethanol) process, with an ethanol production capacity of 100,000 tons per annum, was successfully commissioned in 2017.[8]

Mordenite (MOR) zeolite has been demonstrated to be highly efficient and selective for DME carbonylation to MeOAc.[9−12] The MOR framework features the coexistence of two principal functional channel/cavity, i.e., the unidimensional 12-membered ring (12-MR, 6.5 × 7.0 Å) channels along the *c*-axis and the interconnected side pockets with 8-membered ring windows (8-MR, 3.4 × 4.8 Å).[13−16] The Bronsted acid sites (BASs) located in the 8-MR side pockets have been proved both experimentally and theoretically to be especially active and selective for DME carbonylation.[2,9,17−20] The proposed rationale includes the unique space-confinement effect,[2] the unusual orientation of the transition intermediates,[18] and the local CO aggregation effect associated with the 8-MR side pockets.[21] The 12-MR main channels, nevertheless, are vulnerable to quick coke deposition due to the uncontrolled occurrence of the DME/methanol to hydrocarbon (MTH) reaction, resulting in the blockage of channels and quick catalyst deactivation.

Hitherto, selective removal or passivation of the BASs in the 12-MR channels is the primary tactic to inhibit the occurrence of MTH reaction and enhance the lifetime of MOR zeolite for DME carbonylation.[22,23] However, oriented dealumination of the 12-MR channels is challenging, and the improvement of the catalyst lifetime hitherto reported is rather limited.[24,25] Pyridine modification, a strategy for the selective poisoning of

Received: December 4, 2023
Revised: March 13, 2024
Accepted: March 21, 2024
Published: April 4, 2024

12-MR BASs, has been demonstrated as an effective method to improve catalyst stability.[26,27] Unfortunately, this route increases the complexity of the process and may lead to contamination of the products due to the possible effluent loss of pyridine during the reaction. Considering the toxicity of pyridine, pyridine-free alternatives to improve the catalytic stability of MOR zeolites are desired.

Recently, important progress has been made in modulating the evolution of coke species in the zeolite-catalyzed MTH reaction, achieving a significantly extended catalyst lifetime. Arora et al. first reported that the MTH reaction stability catalyzed by SAPO-34 could be remarkably enhanced (by a factor of 70) by cofeeding high-pressure H_2.[28] They proposed that H_2 functioned as a hydrogen transfer reagent and intercepted the formation pathways of deactivation-inducing polycyclic aromatic hydrocarbons. A further mechanistic study revealed that the higher proclivity of 1,3-butadiene to hydrogenation with H_2 intercepted its further transformation and mitigated the production of the polycyclic species.[29] Our group investigated the positive effect of cofeeding H_2 and H_2O in the MTH reaction over SAPO-34, resulting in a 200-fold increase in methanol processing capacity. This notable enhancement can be attributed to the hydrogenation capacity of the BASs and the consequent retarded formation of heavy aromatic deposits.[30] The above findings illuminate us that the MTH side reactions and the corresponding coking process occurring during the DME carbonylation can potentially be controlled through the coupling of high-pressure H_2 cofeeds.

The incorporation of copper (Cu) into MOR zeolite has been demonstrated by previous studies to enhance the stability and activity of HMOR in DME carbonylation.[31−33] Zhan et al. investigated the reaction mechanism over Cu-HMOR and proposed that Cu^0 plays a pivotal role in promoting DME carbonylation, with a synergetic effect observed between Cu^0 and the neighboring BASs.[34] By incorporating zinc (Zn), Reule et al. successfully synthesized a distinctive 1Cu-4Zn/HMOR catalyst.[35] This specific catalyst features an enhancement of overall MeOAc yield (4×) and catalyst lifespan (6×) when compared to those of the Cu-HMOR counterpart. The steady-state reaction was sustained for ca. 45 h with a MeOAc yield ranging between 0.20 and 0.25 $g{\cdot}g_{cat}^{-1}{\cdot}h^{-1}$. However, it is noteworthy that there remains a pressing need for further enhancement in catalyst stability as the steady reaction lifespan, as it stands, is still far from satisfactory.

In this contribution, we proposed the notion of "benign coke", which involves the intentional cultivation and controlled evolution of coke species in the catalysts, with the aim of it playing a constructive role in catalysis. Drawing on the concept of benign coke, we successfully developed novel MOR-based DME carbonylation catalysts that are distinguished by long-term stability and high activity. This achievement was made possible through the synergy of various factors, including the positive influence of H_2 cofeeds on the regulation of MTH-derived coke formation, the enhanced hydrogenation capacity due to the presence of Cu species, and the selectivity adjustments facilitated by the benign coke. Particularly noteworthy results were obtained with the CuZn-HMOR sample, which has consistently exhibited MeOAc production rates of 0.4−0.5 $g{\cdot}g_{cat}^{-1}{\cdot}h^{-1}$, with MeOAc selectivity exceeding 98% for a duration exceeding 500 h. This represents a remarkable advancement in catalyst longevity, surpassing that of HMOR by a factor of 50+. Both the quantity and characteristics of the deposited coke have a profound impact on the outcomes of benign coke-mediated carbonylation catalysis.

2. EXPERIMENTAL SECTION

2.1. Zeolite Synthesis and Catalyst Preparation. The parent mordenite was synthesized hydrothermally using tetraethylamine hydroxide (TEAOH) as the organic structure directing agents (OSDAs). A typical synthesis procedure is described as follows. Sodium hydroxide, sodium aluminate, TEAOH solution (35 wt %), and H_2O were first mixed at room temperature and stirred until completely dissolved. Subsequently, under vigorous stirring, silica sol (30 wt %) was added dropwise into the above solution. After aging at ambient temperature for 1 h, seed crystals (4 wt % relative to SiO_2) were added, and the mixture underwent further agitation for another 1 h. The molar composition of the obtained reaction gels was as follows: $36SiO_2$: Al_2O_3: $3.0Na_2O$: $3.0(TEA)_2O$: $480H_2O$. The mixture was further transferred into a 100 mL autoclave and crystallized at 170 °C for 48 h under static conditions. After crystallization, the solid product was washed with distilled water, recovered by centrifugation, and dried at 120 °C for 12 h. To remove the encapsulated OSDAs, the as-synthesized sample was heated (1 °C/min) to 550 °C under dry air and kept at this temperature for 4 h. The resultant sample was further transformed to its NH_4 type (NH_4-MOR) by ammonium exchange within 1 M NH_4NO_3 solution (1 h@ 80 °C, repeated 3 times) and proton-type (HMOR) via subsequent calcination at 550 °C for 4 h. The prepared NH_4-HMOR sample was subjected to ion exchange in a 0.2 M solution of copper(II) nitrate (Cu $(NO_3)_2$) at 50 °C for 3 times, drying at 120 °C overnight and a subsequent calcination at 550 °C under air for 6 h, leading to the preparation of Cu-HMOR. Similarly, the prepared NH_4-HMOR sample underwent ion exchange in a solution containing 1 M copper(II) nitrate (Cu $(NO_3)_2$) and 1 M Zinc(II) nitrate (Zn $(NO_3)_2$) at 50 °C for 3 times, drying at 120 °C overnight and subsequent calcination at 550 °C under air for 6 h, leading to the preparation of sample CuZn-HMOR. Before catalytic evaluation, the prepared Cu-HMOR or CuZn-HMOR has to be reduced in an N_2/H_2 mixture (N_2/H_2 = 9). H_2 reduced Cu-HMOR sample is also prepared to follow the variation of Cu species.

2.2. Characterization. The X-ray diffraction (XRD) patterns were obtained on an PANalytical X'Pert PRO X-ray diffractometer using Cu Kα radiation (λ = 0.154059 nm) at 40 kV and 40 mA. The elemental compositions of the samples were determined using a Philips Magix-601 X-ray fluorescence (XRF) spectrometer. The scanning electron microscope (SEM) images and EDX mapping were recorded on a Hitachi SU8020 scanning electron microscope. TEM images were recorded on a JEOL JEM-2100 transmission electron microscope. The N_2 sorption isotherms were measured on a Micromeritics ASAP 2020 analyzer. Based on the Brunauer−Emmett−Teller (BET) method, the total surface area was calculated. The micropore volume and area were derived using the t-plot method. An SDT650 TA analyzer was used for thermogravimetry analysis (TG) from room temperature to 900 °C at a heating rate of 10 °C min^{-1} under an air atmosphere (100 mL min^{-1}). Fourier transform infrared spectra (FTIR) were recorded on a Nicolet IS50 FTIR spectrometer equipped with an MCT detector. The self-supported sample wafers (10 mg) were placed into a quartz cell and pretreated at 350 °C for 1 h under vacuum, and the spectra of the pretreated sample were recorded at room temperature. The organics that remained in the spent zeolites after reaction were analyzed by GC-MS. The spent catalyst (100 mg) was first dissolved in 1 mL of HF solution (40 wt %). The soluble organics in the mixture were extracted with 1 mL CH_2Cl_2 containing 10 ppm of C_2Cl_6 as an internal standard and then analyzed using an Agilent 7890B GC-MS equipped with an HP-5 capillary column. After HF dissolution-CH_2Cl_2 extraction, the insoluble coke suspended in the oil phase or the black particles floating between the aqueous phase and oil phase was recovered by suction filtration, followed by careful purification with CH_2Cl_2 to remove the absorbed organic species. The isolated insoluble coke was measured with MALDI FT-ICR MS. One mg of

https://doi.org/10.1021/acsami.3c18170
ACS Appl. Mater. Interfaces 2024, 16, 18745−18753

the collected insoluble coke was suspended in 200 μL of tetrahydrofuran (THF) with dithranol as MALDI matrix (5 mg mL^{-1} in THF). One μL of the mixture was spotted onto the sample holder. After air drying at room temperature, MS signals were recorded in positive ion mode on a 15-T FT-ICR mass spectrometer (Solarix XR, Bruker Daltonics, Bremen, Germany) equipped with a Nd:YAG laser emitting 355 nm laser to generate ions. Ion source parameters were optimized to a broadband range ($300 < m/z < 1200$) for coke species analysis. Ionization was achieved with 200 Hz, and 32 shots were summated in random handed walk with a grid width of 1000 μm. The mass spectrometer was calibrated before measurement by a peptide calibration standard.

2.3. Catalytic Testing. DME carbonylation evaluation was evaluated in a high-pressure fixed-bed reactor. The H-MOR or Cu/HMOR catalysts (0.2 g, 40−60 mesh) were pretreated in a mixture of N_2 and H_2 (N_2/H_2 = 9, total flow = 25 mL/min) at 300 °C for 2 h. Afterward, the reactor was cooled, and the temperature maintained at 275 °C. A gas mixture with a composition of DME/CO/N_2 = 5/35/60 or DME/CO/H_2 = 5/35/60 was introduced into the reactor at a gas hourly space velocity (GHSV) of 10 000 mL/g/h. The total pressure was 4.0 MPa. The product analysis was carried out using an Agilent 7890B gas chromatograph equipped with a Pora PLOT Q capillary column and an FID detector.

3. RESULTS AND DISCUSSION

3.1. Physiochemical Properties of the Prepared Cu-HMOR Zeolite. Cu species were introduced into the NH_4-form MOR zeolite via a facile liquid ion-exchange process in a Cu $(NO_3)_2$ solution under controlled pH. A subsequent calcination removal of the ammonia under an air atmosphere finalized the preparation of Cu-HMOR with a Cu loading of 2.5 wt % in this study. The XRD pattern, N_2 sorption results, SEM image, and EDX mapping analysis of the prepared Cu-HMOR zeolite are presented in Figure 1. The XRD pattern of

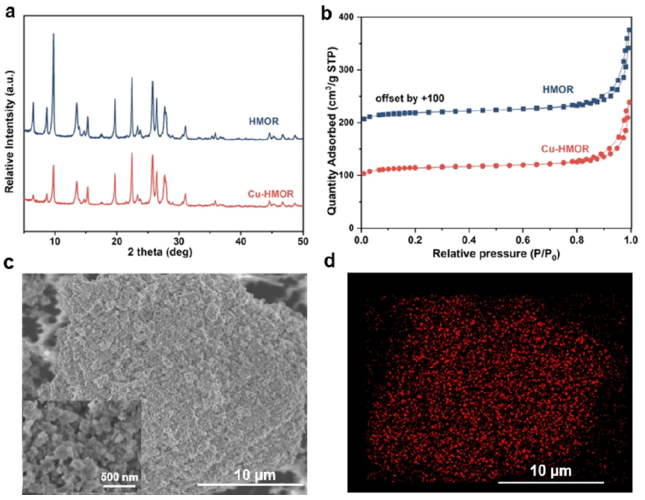

Figure 1. General features of Cu-HMOR and its parent sample HMOR. (a) XRD patterns. (b) N_2 sorption isotherms. (c) SEM image with high-resolution inset to showcase the nanoscale primary particles of the Cu-HMOR agglomerate. (d) EDX mapping of Cu species in Cu-HMOR.

Cu-HMOR displays well-resolved diffraction peaks that could be well-indexed to the MOR structure (Figure 1a). No diffraction due to bulk Cu or copper oxide can be discerned, indicating a high dispersion of Cu species inside the MOR crystals. The N_2 sorption isotherms and the deduced textural properties of Cu-HMOR and its Cu-free counterpart are shown in Figure 1b and Table S1. After Cu introduction, the micropore volume and surface area are only slightly perturbed, excluding the possibility of Cu-induced pore blockage. The SEM image shows that Cu-HMOR is actually a crystal aggregate composed of primary particles of 100−200 nm. EDX mapping (Figures 1c and S1) evidence the highly homogeneous distribution of Cu species. Note that Cu nanoparticles with a size ranging from 2 to 3 nm can be observed in the TEM image of sample Cu-HMOR following H_2 reduction, suggesting that sintering occurs during the reduction process (Figure S1d).

The FTIR spectra in the ν(OH) region (Figure S2) exhibit two prominent bands at 3742 and 3606 cm^{-1}, which correspond to the external silanols and Bronsted acid hydroxyls, respectively. The band at 3606 cm^{-1}, which could be further deconvoluted into two sub-bands at 3610 cm^{-1} (12-MR BASs) and 3585 cm^{-1} (8-MR BASs), exhibits a decrease after Cu introduction in both Cu-HMOR and its reduced counterpart, indicating the anchoring of Cu^{2+} to the Si−O−Al bridge oxygen during Cu^{2+} exchange. It is noteworthy that a larger proportion of Cu cations are anchored in the 8-MR side pockets, as indicated by the enriched 12-MR BAS proportion in the deconvoluted FTIR spectra (Figure S3) and the evidently decreased 8-MR BAS hydroxyls of Cu-HMOR after pyridine sorption at 300 °C (Figure S4).

3.2. Effect of H_2/N_2 Cofeeds on the DME Carbonylation Performance of Cu-HMOR. Figure 2 illustrates the effects of cofeeding H_2 versus N_2 on the activity, lifetime, and product distribution of DME carbonylation on the Cu-HMOR catalyst. When N_2 was cofed, the DME conversion increased rapidly to 73.9% within 5 h but then declined sharply to approximately 6% after 60 h, indicating the poor catalytic stability of Cu-HMOR under an N_2 atmosphere. It is noteworthy that the MeOAc selectivity remained stable at around 98% throughout the postpeak DME conversion period. On the other hand, when H_2 was cofed, the catalyst achieved a peak activity of 53% DME conversion at 2.5 h. The conversion value decreased to 40.4% at 15 h, followed by a quasi-steady DME conversion with a slight decline of 5% until 66 h, indicating a significant improvement in catalytic stability with H_2 cofeeds. However, the MeOAc selectivity during this quasi-steady-state period was only around 35%. The corresponding evolution of effluent products under an H_2 atmosphere (Figure 2d) reveals that the major byproducts were hydrocarbons derived from the MTH reaction. The relatively stable selectivity of hydrocarbons during the quasi-steady-state period suggests that the MTH reaction proceeds in a mild mode with restrained coke depositions. Furthermore, considering the significantly higher CH_4 selectivity under H_2 cofeeds compared to N_2 cofeeds, it is speculated that most of CH_4 is generated from the hydrogenolysis of DME/methanol rather than the MTH reaction.[36] In addition to hydrocarbons, small amounts of methanol and acetic acid can also be observed in the product spectrum. To summarize, significantly improved DME carbonylation catalytic stability was achieved on Cu-HMOR with H_2 cofeeds at the expense of the MeOAc selectivity.

The DME carbonylation of Cu-free HMOR was also investigated under both N_2 and H_2 atmospheres to elucidate the role of the Cu species. The evolution of the DME conversion and MeOAc selectivity is shown in Figure 2b. Similar to Cu-HMOR, under an N_2 atmosphere, a monotonous decline in DME conversion was observed after 1 h. To investigate the possibility of H_2-promoted catalyst regeneration, H_2 cofeeds were introduced after 45 h of reaction.

https://doi.org/10.1021/acsami.3c18170
ACS Appl. Mater. Interfaces 2024, 16, 18745−18753

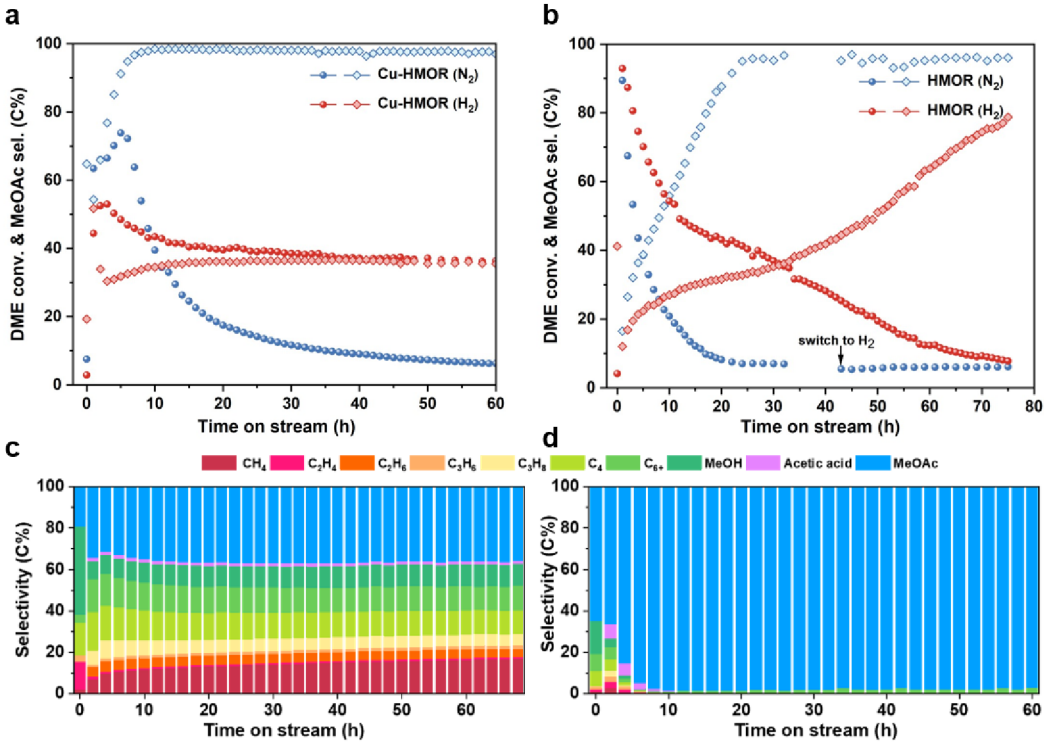

Figure 2. (a, b) DME conversion (solid symbols) and MeOAc selectivity (open symbols) on Cu-HMOR and HMOR with N_2/H_2 cofeeds in DME carbonylation reaction. (c, d) Detailed product selectivity versus time on stream on Cu-HMOR with H_2 and N_2 cofeeds, respectively. Reaction conditions: 275 °C, 200 KPa DME, 1.4 MPa CO, 2.4 MPa H_2 or N_2, GHSV = 10000 mL·g_{cat}^{-1}·h^{-1}.

However, activity regeneration was rather limited. When the reaction was conducted under an H_2 atmosphere, the deactivation phenomenon was alleviated, but it was still more severe than on Cu-HMOR (H_2). These results demonstrate the indispensable role of Cu in the H_2-promoted improvement of catalyst stability. The insufficient hydrogenation ability of the BASs on the HMOR, which differs from the findings by Arora et al. and our previous study,[28,30] can be attributed to the lower reaction temperature employed for DME carbonylation, which necessitates the presence of metals such as Cu that can help dissociate H_2 at lower temperatures.

3.3. DME Carbonylation on Coke-Mediated Cu-HMOR. The preserved high MeOAc selectivity during the postpeak DME conversion period on Cu-HMOR under an N_2 atmosphere suggests that coke deposition might be beneficial for mitigating the MTH reaction (Figure 2a,d). On the other hand, the improved catalytic stability of Cu-HMOR under an H_2 atmosphere implies the potent effect of H_2 cofeeds in controlling coke deposition from the MTH reaction (Figure 2a,c). Consequently, a two-step reaction procedure was formulated for the Cu-HMOR catalyst. This procedure entails: (I) initiating the reaction under a DME-CO-N_2 stream for a brief period, during which coke species are rapidly deposited onto the catalyst, thereby enhancing MeOAc selectivity; (II) switching from N_2 cofeeds to H_2 cofeeds to ameliorate catalyst stability.

A typical reaction procedure is as follows. Initially, Cu-HMOR was exposed to a DME-CO-N_2 stream at 275 °C and 4 MPa total pressure for a duration of 36 h, hereinafter referred to as Cu-HMOR/C-36h. Subsequently, a swift transition to a DME-CO-H_2 feedstock was initiated. During the initial stage (I) (Figure S5), a characteristic roller coaster-style curve was observed, wherein the DME conversion exhibited a continuous decline, reaching 15% within 36 h. Following the transition to an H_2 atmosphere (II) (Figure 3a), a progressive rebuild-up in catalytic activity was evident, with DME conversion gradually increasing from 15% to 30% over a span of 70 h. It is postulated that this rejuvenation in activity, induced by the introduction of H_2, can be attributed to H_2-facilitated coke removal and subsequent enhancement of catalyst diffusion properties. Notably, a sustained period of stable reaction lasting over 100 h was observed before the experiment was terminated (TOS = 70−172 h, with DME conversion remaining in the range of 30−34%). This phenomenon highlights the effectiveness of H_2 cofeeds in effectively managing coke deposition on Cu-HMOR.

During the reaction period under an H_2 atmosphere, the MeOAc selectivity remained higher than 97.5%, which is noticeably different from the outcomes observed when employing fresh Cu-HMOR catalyst with H_2 cofeeds (refer to Figure 2). This marked distinction highlights the advantageous role of the intentionally constructed coke species in mitigating the MTH reaction and fine-tuning the selectivity toward MeOAc. Remarkably, the steady-state MeOAc yield on Cu-HMOR/C-36h reached 0.55 g·g_{cat}^{-1}·h^{-1}, a metric that stands among the highest reported values in the literature (Table S2).[22,23,35] The evolution of the byproducts is illustrated in Figure S6. Hydrocarbons, resulting from the MTH reaction, are the predominant byproducts. Additionally, trace amounts of methanol and acetic acid can also be observed, stemming from the inevitable generation of water molecules in the MTH process.

3.4. The Impact of Precoking Duration on DME Carbonylation. Two additional samples with reduced precoking durations, denoted as Cu-HMOR/C-24h and Cu-HMOR/C-15h, were also prepared to investigate the potential

https://doi.org/10.1021/acsami.3c18170
ACS Appl. Mater. Interfaces 2024, 16, 18745−18753

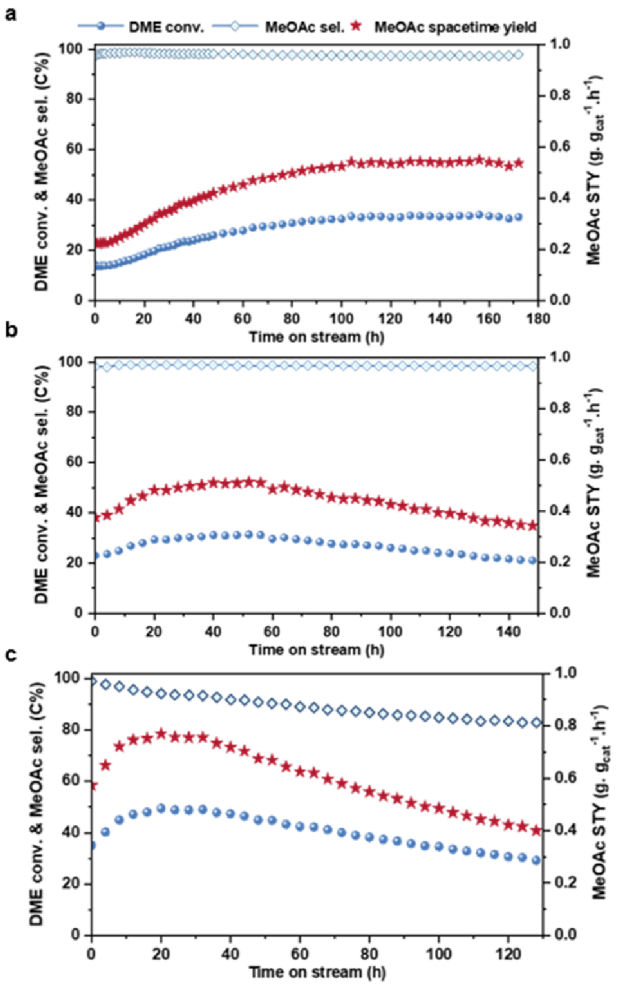

Figure 3. DME carbonylation performance on the precoked catalysts: (a) Cu-HMOR/C-36h, (b) Cu-HMOR/C-24h, and (c) Cu-HMOR/C-15h under H_2 cofeeds. Reaction conditions: 275 °C, 200 KPa DME, 1.4 MPa CO, 2.4 MPa H_2, GHSV = 10000 mL·g$_{cat}^{-1}$·h^{-1}.

impact of varied precoking extents on the catalytic performance of Cu-HMOR on DME carbonylation (Figure 3b,c).

For the sample with the shortest precoking time (Cu-HMOR/C-15h), following the switch to an H_2 atmosphere, the DME conversion was quickly regained to 50% at 22 h. Subsequently, a linear decline ensued, ultimately reaching 29.2% by 128 h. Concurrently, the selectivity of MeOAc gradually decreased from 98% to 83%. Meanwhile, the selectivities of byproducts (Figure S5), including hydrocarbons, methanol, and acetic acid, exhibited an increasing trend over time, while the reaction proceeded. These findings strongly suggest that the contribution of the MTH reaction on Cu-HMOR/C-15h progressively escalates as the reaction time is extended under an H_2 atmosphere. For Cu-HMOR/C-24h, the DME conversion under an H_2 atmosphere was recovered to 31.5% at 77 h and declined slowly afterward to 22.7% at 127 h. The MeOAc selectivity remained relatively stable at around 98%, indicating the continued dominance of the carbonylation reaction.

The distinct catalytic behaviors observed among samples with different precoking durations imply that the degree of precoking, including both the quantity and the nature of precoking species, should be pivotal in the coke-mediated DME carbonylation reaction. This observation prompts us to further delve into the quantitative and qualitative evolution of coke species in the subsequent sections.

3.5. Coke Contents Before and After Cofeeding H_2.

The evolution of the coke content on the Cu-HMOR catalysts is investigated by thermal analysis. Figure S7 presents the corresponding TG-DSC curves, while Figure 4 provides a succinct summary of the results.

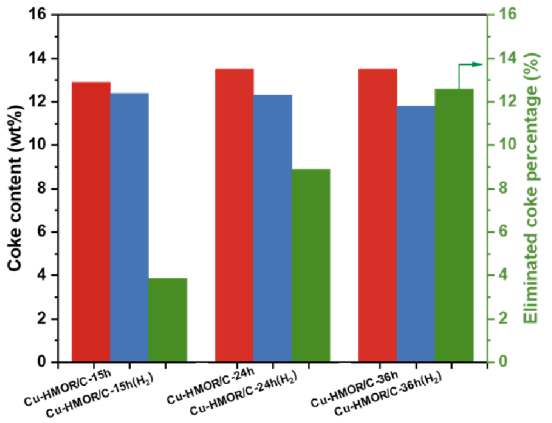

Figure 4. Coke contents on Cu-HMOR with different precoking times (red), the variation after DME carbonylation reaction within H_2 cofeeds (blue), and the percentages of eliminated coke (green).

Before transitioning to an H_2 atmosphere, the quantification of carbonaceous deposits accumulated on the samples yielded values of 12.9, 13.5, and 13.5 wt % for Cu-HMOR/C-15h, Cu-HMOR/C-24h, and Cu-HMOR/C-36h, respectively. Subsequently, by extending the precoking time to 60 h (denoted as Cu-HMOR/C-60h) until the DME conversion reached a mere 6%, only a negligible amount of coke (0.1 wt %) was further gained. These results unequivocally establish that Cu-HMOR reached a state of quantitative saturation with carbonaceous deposits following a 24-h precoking process.

Upon reaction within H_2 cofeeds, the coke contents exhibited a noticeable decline for all the investigated samples, providing compelling evidence that cofeeding H_2 can effectively inhibit coke deposition and eliminate pre-existing coke species. The removed coke contents constitute 3.9%, 8.9%, and 12.6% of the total coke present in the samples. This elimination is expected to enhance the accessibility of active sites and, consequently, boost the recovery of activity. Moreover, the higher coke elimination rate observed for the samples with prolonged precoking duration (Figure S7) suggests that the coke species formed during a longer reaction time under N_2 are more readily eliminated.

3.6. Coke Species Before and After Cofeeding H_2.

Combined techniques (GC-MS and MALDI FT-ICR MS) were employed to get a better understanding of the coke species present on the catalysts. The deposited coke species, in the samples before and after reaction in an H_2 atmosphere, were liberated by hydrofluoric acid (HF) dissolution followed by CH_2Cl_2 extraction. The extracted carbonaceous species were analyzed by GC-MS, and the corresponding chromatograms are depicted in Figure 5a.

Before cofeeding H_2, methylated benzenes, closely related to the hydrocarbon-pool active species in the MTH reaction, dominate the spectra. Their quantities exhibit a declining trend with prolonged precoking time, in congruence with the diminishing MTH reaction activity. In addition to methylated

https://doi.org/10.1021/acsami.3c18170
ACS Appl. Mater. Interfaces 2024, 16, 18745−18753

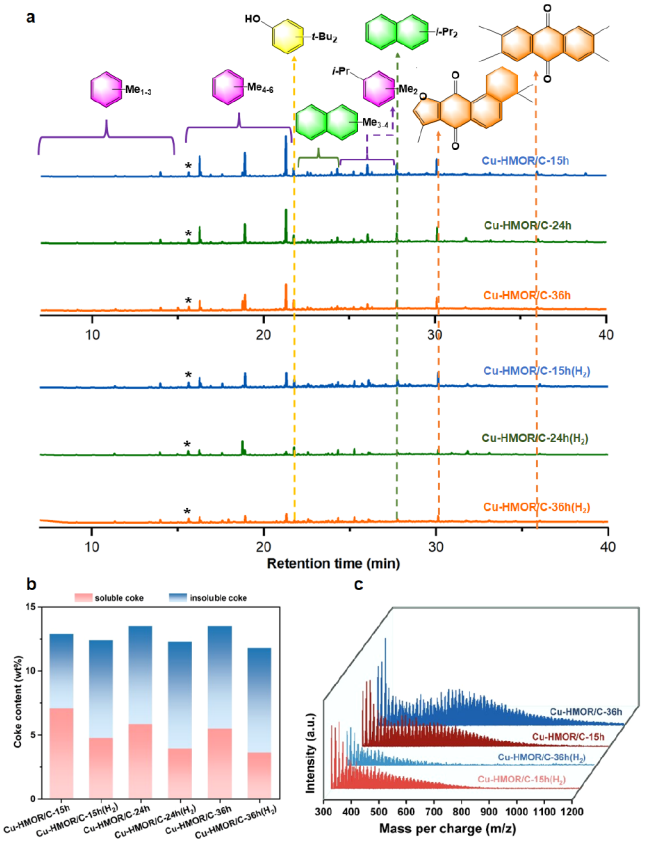

Figure 5. Analyses of soluble and insoluble coke species retained in Cu-HMOR/C-15h, Cu-HMOR/C-24h, and Cu-HMOR/C-36h before and after DME carbonylation reaction with H_2 cofeeds. (a) shows GC-MS spectra of the CH_2Cl_2-soluble carbonaceous species. The asterisk labeled peak corresponds to the internal C_2Cl_6 standard, and all the chromatograms were normalized by the internal standard. (b) The contents of soluble and insoluble coke retained in the catalysts. (c) MALDI FT-ICR mass spectra of the insoluble coke deposits in the catalysts.

benzenes, more substantial aromatic compounds, such as alkylated naphthalenes, were observed. Furthermore, a range of oxygen-containing aromatics, including phenols and diones, which seldom appear in the MTH reaction, was also discerned. The high concentration of CO within the atmosphere and the potential occurrence of carbonylation could offer plausible explanations for the formation of oxygen-containing aromatic compounds. After cofeeding H_2, there is a discernible reduction in the overall intensities of the chromatogram peaks. This reduction suggests a decrease in the fraction of CH_2Cl_2-soluble coke within the spent catalysts, which should be attributed to either H_2-assisted coke elimination or their subsequent transformation into bulkier, insoluble coke forms.

The masses of soluble and insoluble coke species before and after cofeeding H_2, along with their relative percentages, were calculated to gain further insights into this process. The total coke contents of the catalysts were determined by TGA (Figure 4). The contents of soluble coke were determined, based on a protocol developed within our laboratory, using C_2Cl_6 as an internal standard.[37] As illustrated in Figure 5b, the quantity of insoluble coke on the catalyst increases with the precoking time, while the amount of soluble coke decreases, indicating a gradual transformation of soluble coke into insoluble coke. This phenomenon can be understood by acknowledging that insoluble coke is known to develop through the extension and clustering of the soluble coke. Upon transitioning to H_2 cofeeds, all three catalysts exhibit a further increase in the amount of insoluble coke and a concurrent decrease in soluble coke. This clearly demonstrates that the presence of H_2 cannot eliminate the transformation of soluble coke to insoluble coke.

Since GC-MS is limited to the detection of molecules with a maximum molecular weight (MW) of 300, we conducted further analysis on the heavier carbonaceous deposits (MW from 300 to 1200) present in the CH_2Cl_2 extracts of Cu-HMOR-C/15h and Cu-HMOR/C-36h using MALDI FT-ICR MS (Figure 5c). Although the intricate spectra pose challenges for the precise determination of the specific chemical formula of the encapsulated coke species, the variation trend of the polymerization degree of the coke species is clear. Before cofeeding H_2, there is a noticeable increase in the percentage of coke species exhibiting higher polymerization degrees with the extension of the precoking duration. This evolution of coke species is in congruence with the decreased DME carbonylation activity, suggesting that the development of larger-sized coke depositions and the consequent deterioration of mass transfer properties likely constitute the primary reasons for the rapid deactivation of Cu-HMOR under an N_2 atmosphere. After transitioning to an H_2 atmosphere, the proportion of coke species with a higher polymerization degree clearly declines for both investigated samples. This phenomenon highlights the H_2-mediated reduction in ultralarge coke species. This outcome is rational, as coke species characterized by an increased degree of polymerization have been recognized

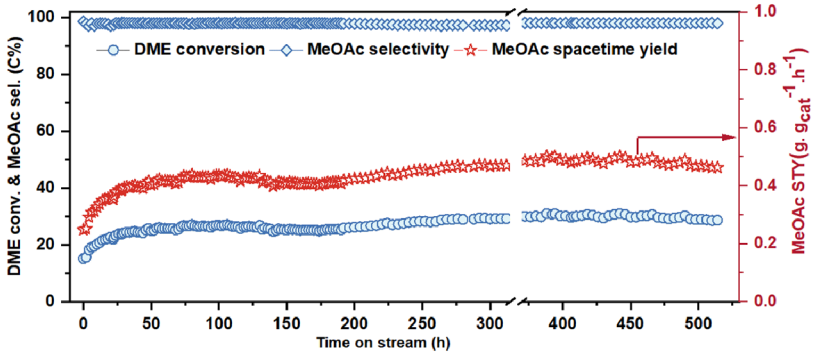

Figure 6. DME carbonylation performance on CuZn-HMOR/C-26h with H_2 cofeeds. Reaction conditions: 275 °C, 200 KPa DME, 1.4 MPa CO, 2.4 MPa H_2, GHSV = 10000 mL·g_{cat}^{-1}·h^{-1}.

https://doi.org/10.1021/acsami.3c18170
ACS Appl. Mater. Interfaces 2024, 16, 18745−18753

as more susceptible to hydrocracking when exposed to an H_2 atmosphere.[38] However, as illustrated in Figure 5b, the proportion of insoluble coke increased even when H_2 was cofed. Therefore, it can be deduced that, although incapable of completely suppressing the transformation of soluble coke into insoluble coke, cofeeding H_2 can effectively inhibit the formation of ultralarge coke species, which are more detrimental to the mass transfer properties and pivotal for the catalyst deactivation.

In summary, both the quantity and nature of the precoking species, the presence of H_2 atmosphere, and the incorporation of metal species with hydrogenation capability are all pivotal factors contributing to the benign coke-mediated strategy in achieving extended lifespan in the DME carbonylation reaction.

3.7. DME Carbonylation on Coke-Mediated CuZn-HMOR. In consideration of the well-acknowledged beneficial effect of Zn additives on Cu dispersion in methanol synthesis catalysts as well as Cu-modified HMOR catalysts,[35] HMOR catalysts modified by both Cu and Zn, featuring a comparable Cu/Zn loading of ca. 1.8 wt % were also prepared and assessed for their performance in the coke-mediated DME carbonylation reaction. Before initiating the catalytic reaction under an H_2 atmosphere, the sample underwent exposure to a DME-CO-N_2 stream for 26 h and was hereafter denoted as CuZn-HMOR/C-26h. From Figure 6, the DME conversion on CuZn-HMOR/C-26h was well preserved with no obvious decline until the end of the reaction (TOS = 514 h). Notably, a sustained steady-state reaction period, characterized by a plateau conversion of approximately 30%, spanned over 520 h, while the selectivity toward MeOAc remained consistently above 98%. In stark contrast, the DME conversion was observed to decline sharply to 20% in just 10 h for HMOR under an N_2 atmosphere (Figure 2b). The longevity of CuZn-HMOR was significantly enhanced by a factor of 50+ compared to HMOR. Meanwhile, the MeOAc yield during the steady period was calculated to fluctuate between 0.4 and 0.5 $g{\cdot}g_{cat}^{-1}{\cdot}h^{-1}$. Notably, the MeOAc yield achieved here ranks among the highest values ever reported for MOR-based DME carbonylation catalysts, particularly when employing a pyridine-free route. More importantly, the steady production of MeOAc at such a high rate was sustained for an unprecedented period of over 520 h, which has never been documented in previous literature (refer to Table S2), demonstrating the practical application potential of our proposed strategy.

TEM images (Figure S9) of the spent CuZn-HMOR/C-26h and Cu-HMOR/C-36h after the DME carbonylation reaction were measured to monitor the variations of the metal species. Although a discernible agglomeration phenomenon was observed in both samples, the extent of agglomeration was markedly less severe in CuZn-HMOR. The average size of the agglomerated Cu for CuZn-HMOR after reaction for over 520 h is even smaller than Cu-HMOR after reaction for 172 h. The DME carbonylation result of CuZn-HMOR further confirms the efficacy of the coke-mediated DME carbonylation strategy. The nature and quantity of the incorporated metals were expected to influence the hydrogenation capacity, thereby impacting the balance between coke formation from MTH and coke elimination through hydrocracking. These factors, in turn, have a significant influence on the selectivity toward MeOAc and, more importantly, on long-term catalytic stability.

4. CONCLUSION

In this work, the positive effects of coke in catalysis were unveiled and are exemplified in DME carbonylation. We demonstrated that coke can be controlled and beneficially utilized: (i) Unlike the typical uncontrollable coke formation, we managed to control its formation in a benign manner; (ii) contrary to its usual detrimental impact, benign coke is beneficial for the catalytic performance amelioration. Based on the proposed concept of benign coke, novel DME carbonylation catalysts with long-term stability and high activity were created by combining the contributions of H_2 cofeeds and Cu species in the regulation of MTH-derived coke, and the product selectivity adjustment by the benign coke. Detailed analysis revealed that ultralarge coke species can be effectively eliminated by the present strategy, which would facilitate the mass transfer within the catalyst; the residual coke with a relatively low polymerization degree mitigates the uncontrolled occurrence of MTH reaction. The most highlighted DME carbonylation results were achieved on CuZn-HMOR, which exhibits a steady MeOAc yield of 0.4−0.5 $g_{MeOAc}{\cdot}g_{cat}^{-1}{\cdot}h^{-1}$ for over 520 h and a remarkable longevity enhanced by a factor of over 50 compared to HMOR, demonstrating industrial application potential. The current work not only provides valuable insights into the control of coke formation in DME carbonylation but also inspires further research into other reactions that could be potentially improved by this benign coke strategy.

■ ASSOCIATED CONTENT

Supporting Information

The Supporting Information is available free of charge at https://pubs.acs.org/doi/10.1021/acsami.3c18170.

Supplementary figures including SEM/EDX, FTIR, additional catalytic evaluation results, TG-DSC curves, and calculated coke elimination rate TEM, summarized textural properties, and a summary of reported MeOAc spacetime yield and catalyst lifetime in MOR-catalyzed DME carbonylation (PDF)

■ AUTHOR INFORMATION

Corresponding Authors

Peng Tian − *National Engineering Research Center of Lower-Carbon Catalysis Technology, Dalian National Laboratory for Clean Energy, Dalian Institute of Chemical Physics, Chinese Academy of Sciences, Dalian 116023, China;* orcid.org/0000-0002-8768-0154; Email: tianpeng@dicp.ac.cn

Zhongmin Liu − *National Engineering Research Center of Lower-Carbon Catalysis Technology, Dalian National Laboratory for Clean Energy, Dalian Institute of Chemical Physics, Chinese Academy of Sciences, Dalian 116023, China;* orcid.org/0000-0002-7999-2940; Email: liuzm@dicp.ac.cn

Authors

Dong Fan − *National Engineering Research Center of Lower-Carbon Catalysis Technology, Dalian National Laboratory for Clean Energy, Dalian Institute of Chemical Physics, Chinese Academy of Sciences, Dalian 116023, China;* orcid.org/0000-0002-8815-0163

Nan Chen − *National Engineering Research Center of Lower-Carbon Catalysis Technology, Dalian National Laboratory*

https://doi.org/10.1021/acsami.3c18170
ACS Appl. Mater. Interfaces 2024, 16, 18745−18753

for Clean Energy, Dalian Institute of Chemical Physics, Chinese Academy of Sciences, Dalian 116023, China; University of Chinese Academy of Sciences, Chinese Academy of Sciences, Beijing 100049, China

Songyue Han − *National Engineering Research Center of Lower-Carbon Catalysis Technology, Dalian National Laboratory for Clean Energy, Dalian Institute of Chemical Physics, Chinese Academy of Sciences, Dalian 116023, China; University of Chinese Academy of Sciences, Chinese Academy of Sciences, Beijing 100049, China*

Lingyun Li − *National Engineering Research Center of Lower-Carbon Catalysis Technology, Dalian National Laboratory for Clean Energy, Dalian Institute of Chemical Physics, Chinese Academy of Sciences, Dalian 116023, China*

Nan Wang − *National Engineering Research Center of Lower-Carbon Catalysis Technology, Dalian National Laboratory for Clean Energy, Dalian Institute of Chemical Physics, Chinese Academy of Sciences, Dalian 116023, China*

Wenhao Cui − *National Engineering Research Center of Lower-Carbon Catalysis Technology, Dalian National Laboratory for Clean Energy, Dalian Institute of Chemical Physics, Chinese Academy of Sciences, Dalian 116023, China; University of Chinese Academy of Sciences, Chinese Academy of Sciences, Beijing 100049, China*

Quanyi Wang − *National Engineering Research Center of Lower-Carbon Catalysis Technology, Dalian National Laboratory for Clean Energy, Dalian Institute of Chemical Physics, Chinese Academy of Sciences, Dalian 116023, China*

Complete contact information is available at: https://pubs.acs.org/10.1021/acsami.3c18170

Author Contributions

The manuscript was written through the contributions of all authors. All authors have given approval to the final version of the manuscript.

Notes

The authors declare no competing financial interest.

■ ACKNOWLEDGMENTS

This work is supported by the National Natural Science Foundation of China (Nos. 22272173, 21991090, 21991091, and 22288101), the National Key R&D Program of China (2022YFE0116000), and DICP funding (DICP 1202420). The authors thanks to the funding from the Sino-French IRN (International Research Network).

■ REFERENCES

(1) Cheung, P.; Bhan, A.; Sunley, G. J.; Iglesia, E. Selective Carbonylation of Dimethyl Ether to Methyl Acetate Catalyzed by Acidic Zeolites. *Angew. Chem., Int. Ed.* **2006**, *45* (10), 1617−1620.

(2) Bhan, A.; Allian, A. D.; Sunley, G. J.; Law, D. J.; Iglesia, E. Specificity of Sites within Eight-membered Ring Zeolite Channels for Carbonylation of Methyls to Acetyls. *J. Am. Chem. Soc.* **2007**, *129* (16), 4919−4924.

(3) Rasmussen, D. B.; Christensen, J. M.; Temel, B.; Studt, F.; Moses, P. G.; Rossmeisl, J.; Riisager, A.; Jensen, A. D. Reaction Mechanism of Dimethyl Ether Carbonylation to Methyl Acetate over Mordenite a Combined DFT/Experimental Study. *Catal. Sci. Technol.* **2017**, *7* (5), 1141−1152.

(4) Rasmussen, D. B.; Christensen, J. M.; Temel, B.; Studt, F.; Moses, P. G.; Rossmeisl, J.; Riisager, A.; Jensen, A. D. Ketene as a Reaction Intermediate in the Carbonylation of Dimethyl Ether to Methyl Acetate over Mordenite. *Angew. Chem., Int. Ed.* **2015**, *54* (25), 7261−7264.

(5) Diemer, R. B.; Luyben, W. L. Design and Control of a Methyl Acetate Process Using Carbonylation of Dimethyl Ether. *Ind. Eng. Chem. Res.* **2010**, *49* (23), 12224−12241.

(6) Han, S. Y.; Fan, D.; Chen, N.; Cui, W. H.; He, L. H.; Tian, P.; Liu, Z. M. Efficient Conversion of Syngas into Ethanol by Tandem Catalysis. *ACS Catal.* **2023**, *13* (16), 10651−10660.

(7) Zhou, W.; Kang, J. C.; Cheng, K.; He, S.; Shi, J. Q.; Zhou, C.; Zhang, Q. H.; Chen, J. C.; Peng, L. M.; Chen, M. S.; Wang, Y. Direct Conversion of Syngas into Methyl Acetate, Ethanol, and Ethylene by Relay Catalysis via the Intermediate Dimethyl Ether. *Angew. Chem., Int. Ed.* **2018**, *57* (37), 12012−12016.

(8) Grad, P. Debut of a Coal-to-ethanol Plant. https://www.chemengonline.com/debut-coal-ethanol-plant/.

(9) Chen, N.; Zhang, J.; Gu, Y. T.; Zhang, W. N.; Cao, K. P.; Cui, W. H.; Xu, S. T.; Fan, D.; Tian, P.; Liu, Z. M. Designed Synthesis of MOR Zeolites using Gemini-type Bis(methylpyrrolidinium) Dications as Structure Directing Agents and their DME Carbonylation Performance. *J. Mater. Chem. A* **2022**, *10* (15), 8334−8343.

(10) Cao, K. P.; Fan, D.; Gao, M. B.; Fan, B. H.; Chen, N.; Wang, L. Y.; Tian, P.; Liu, Z. M. Recognizing the Important Role of Surface Barriers in MOR Zeolite Catalyzed DME Carbonylation Reaction. *ACS Catal.* **2022**, *12* (1), 1−7.

(11) Cao, K. P.; Fan, D.; Zeng, S.; Fan, B. H.; Chen, N.; Gao, M. B.; Zhu, D. L.; Wang, L. Y.; Tian, P.; Liu, Z. M. Organic-free Synthesis of MOR Nanoassemblies with Excellent DME Carbonylation Performance. *Chin. J. Catal.* **2021**, *42* (9), 1468−1477.

(12) Liu, Y. H.; Zhao, N.; Xian, H.; Cheng, Q. P.; Tan, Y. S.; Tsubaki, N.; Li, X. G. Facilely Synthesized H-Mordenite Nanosheet Assembly for Carbonylation of Dimethyl Ether. *ACS Appl. Mater. Inter.* **2015**, *7* (16), 8398−8403.

(13) Yi, X.; Xiao, Y.; Li, G.; Liu, Z.; Chen, W.; Liu, S.-B.; Zheng, A. From One to Two: Acidic Proton Spatial Networks in Porous Zeolite Materials. *Chem. Mater.* **2020**, *32* (3), 1332−1342.

(14) Chen, W.; Li, G.; Yi, X.; Day, S. J.; Tarach, K. A.; Liu, Z.; Liu, S.-B.; Edman Tsang, S. C.; Góra-Marek, K.; Zheng, A. Molecular Understanding of the Catalytic Consequence of Ketene Intermediates under Confinement. *J. Am. Chem. Soc.* **2021**, *143* (37), 15440−15452.

(15) Gong, K.; Liu, Z.; Liang, L.; Zhao, Z.; Guo, M.; Liu, X.; Han, X.; Bao, X.; Hou, G. Acidity and Local Confinement Effect in Mordenite Probed by Solid-State NMR Spectroscopy. *J. Phys. Chem. Lett.* **2021**, *12* (9), 2413−2422.

(16) Cheng, Z. Z.; Huang, S. Y.; Li, Y.; Cai, K.; Wang, Y.; Wang, M. Y.; Lv, J.; Ma, X. B. Role of Bronsted Acid Sites within 8-MR of Mordenite in the Deactivation Roadmap for Dimethyl Ether Carbonylation. *ACS Catal.* **2021**, *11* (9), 5647−5657.

(17) Cheung, P.; Bhan, A.; Sunley, G. J.; Law, D. J.; Iglesia, E. Site Requirements and Elementary Steps in Dimethyl Ether Carbonylation Catalyzed by Acidic Zeolites. *J. Catal.* **2007**, *245* (1), 110−123.

(18) Boronat, M.; Martinez-Sanchez, C.; Law, D.; Corma, A. Enzyme-like Specificity in Zeolites: A Unique Site Position in Mordenite for Selective Carbonylation of Methanol and Dimethyl Ether with CO. *J. Am. Chem. Soc.* **2008**, *130* (48), 16316−16323.

(19) Li, Y.; Huang, S. Y.; Cheng, Z. Z.; Cai, K.; Li, L. D.; Milan, E.; Lv, J.; Wang, Y.; Sun, Q.; Ma, X. B. Promoting the Activity of Ce-incorporated MOR in Dimethyl Ether Carbonylation through Tailoring the Distribution of Bronsted acids. *Appl. Catal. B* **2019**, *256*, 117777.

(20) Boronat, M.; Martínez, C.; Corma, A. Mechanistic Differences between Methanol and Dimethyl Ether Carbonylation in Side Pockets and Large Channels of Mordenite. *Phys. Chem. Chem. Phys.* **2011**, *13* (7), 2603−2612.

(21) Liu, Z. Q.; Yi, X. F.; Wang, G. R.; Tang, X. M.; Li, G. C.; Huang, L.; Zheng, A. M. Roles of 8-ring and 12-ring Channels in Mordenite for Carbonylation Reaction: From the Perspective of Molecular Adsorption and Diffusion. *J. Catal.* **2019**, *369*, 335−344.

(22) Liu, R.; Fan, B.; Zhi, Y.; Liu, C.; Xu, S.; Yu, Z.; Liu, Z. Dynamic Evolution of Aluminum Coordination Environments in Mordenite Zeolite and Their Role in the Dimethyl Ether (DME) Carbonylation Reaction. *Angew. Chem., Int. Ed.* **2022**, *61* (42), No. e202210658.

(23) Liu, R.; Zeng, S.; Sun, T.; Xu, S.; Yu, Z.; Wei, Y.; Liu, Z. Selective Removal of Acid Sites in Mordenite Zeolite by Trimethylchlorosilane Silylation to Improve Dimethyl Ether Carbonylation Stability. *ACS Catal.* **2022**, *12* (8), 4491−4500.
(24) Wang, X.; Li, R.; Yu, C.; Liu, Y.; Zhang, L.; Xu, C.; Zhou, H. Enhancing the Dimethyl Ether Carbonylation Performance over Mordenite Catalysts by Simple Alkaline Treatment. *Fuel* **2019**, *239*, 794−803.
(25) Xue, H. F.; Huang, X. M.; Zhan, E. S.; Ma, M.; Shen, W. J. Selective Dealumination of Mordenite for Enhancing its Stability in Dimethyl Ether Carbonylation. *Catal. Commun.* **2013**, *37*, 75−79.
(26) Cao, K. P.; Fan, D.; Li, L. Y.; Fan, B. H.; Wang, L. Y.; Zhu, D. L.; Wang, Q. Y.; Tian, P.; Liu, Z. M. Insights into the Pyridine-Modified MOR Zeolite Catalysts for DME Carbonylation. *ACS Catal.* **2020**, *10* (5), 3372−3380.
(27) Liu, J. L.; Xue, H. F.; Huang, X. M.; Wu, P. H.; Huang, S. J.; Liu, S. B.; Shen, W. J. Stability Enhancement of H-Mordenite in Dimethyl Ether Carbonylation to Methyl Acetate by Pre-adsorption of Pyridine. *Chin. J. Catal.* **2010**, *31* (7), 729−738.
(28) Arora, S. S.; Ieskens, D. L. S.; Malek, A.; Bhan, A. Lifetime Improvement in Methanol-to-olefins Catalysis over Chabazite Materials by High-pressure H_2 Co-feeds. *Nat. Catal.* **2018**, *1* (9), 666−672.
(29) Arora, S. S.; Shi, Z. C.; Bhan, A. Mechanistic Basis for Effects of High-Pressure H_2 Cofeeds on Methanol-to-Hydrocarbons Catalysis over Zeolites. *ACS Catal.* **2019**, *9* (7), 6407−6414.
(30) Zhao, X. B.; Li, J. Z.; Tian, P.; Wang, L. Y.; Li, X. F.; Lin, S. F.; Guo, X. W.; Liu, Z. M. Achieving a Superlong Lifetime in the Zeolite-Catalyzed MTO Reaction under High Pressure: Synergistic Effect of Hydrogen and Water. *ACS Catal.* **2019**, *9* (4), 3017−3025.
(31) Wang, S.; Guo, W.; Zhu, L.; Wang, H.; Qiu, K.; Cen, K. Methyl Acetate Synthesis from Dimethyl Ether Carbonylation over Mordenite Modified by Cation Exchange. *J. Phys. Chem. C* **2015**, *119* (1), 524−533.
(32) Zhan, H.; Huang, S.; Li, Y.; Lv, J.; Wang, S.; Ma, X. Elucidating the Nature and Role of Cu species in Enhanced Catalytic Carbonylation of Dimethyl Ether over Cu/H-MOR. *Catal. Sci. Technol.* **2015**, *5* (9), 4378−4389.
(33) Blasco, T.; Boronat, M.; Concepción, P.; Corma, A.; Law, D.; Vidal-Moya, J. A. Carbonylation of Methanol on Metal−Acid Zeolites: *Evidence For a Mechanism Involving a Multisite Active Center*. *Angew. Chem.* **2007**, *46* (21), 3938−3941.
(34) Zhan, H. M.; Huang, S. Y.; Li, Y.; Lv, J.; Wang, S. P.; Ma, X. B. Elucidating the Nature and Role of Cu Species in Enhanced Catalytic Carbonylation of Dimethyl Ether over Cu/H-MOR. *Catal. Sci. Technol.* **2015**, *5* (9), 4378−4389.
(35) Reule, A. A. C.; Semagina, N. Zinc Hinders Deactivation of Copper-Mordenite: Dimethyl Ether Carbonylation. *ACS Catal.* **2016**, *6* (8), 4972−4975.
(36) Zhao, W.; Zhang, B.; Wang, G.; Guo, H. Methane Formation Route in the Conversion of Methanol to Hydrocarbons. *J. Energy Chem.* **2014**, *23* (2), 201−206.
(37) Wang, N.; Zhi, Y. C.; Wei, Y. X.; Zhang, W. N.; Liu, Z. Q.; Huang, J. D.; Sun, T. T.; Xu, S. T.; Lin, S. F.; He, Y. L.; et al.etal. Molecular Elucidating of an Unusual Growth Mechanism for Polycyclic Aromatic Hydrocarbons in Confined Space. *Nat. Commun.* **2020**, *11* (1), 1079.
(38) Jong, S.-J.; Pradhan, A. R.; Wu, J.-F.; Tsai, T.-C.; Liu, S.-B. On the Regeneration of Coked H-ZSM-5 Catalysts. *J. Catal.* **1998**, *174* (2), 210−218.

https://doi.org/10.1021/acsami.3c18170
ACS Appl. Mater. Interfaces 2024, 16, 18745−18753